SERS and Boron Nitride

Deutsche Ausgabe: DOI: 10.1002/ange.201600517
Internationale Ausgabe: DOI: 10.1002/anie.201600517

Boron Nitride Nanosheets Improve Sensitivity and Reusability of Surface-Enhanced Raman Spectroscopy

Qiran Cai, Srikanth Mateti, Wenrong Yang, Rob Jones, Kenji Watanabe, Takashi Taniguchi, Shaoming Huang, Ying Chen, and Lu Hua Li**

Abstract: *Surface enhanced Raman spectroscopy (SERS) is a useful multidisciplinary analytic technique. However, it is still a challenge to produce SERS substrates that are highly sensitive, reproducible, stable, reusable, and scalable. Herein, we demonstrate that atomically thin boron nitride (BN) nanosheets have many unique and desirable properties to help solve this challenge. The synergic effect of the atomic thickness, high flexibility, stronger surface adsorption capability, electrical insulation, impermeability, high thermal and chemical stability of BN nanosheets can increase the Raman sensitivity by up to two orders, and in the meantime attain long-term stability and extraordinary reusability not achievable by other materials. These advances will greatly facilitate the wider use of SERS in many fields.*

Surface enhanced Raman spectroscopy (SERS) is one of a few analytical techniques with single-molecule sensitivity,[1] and has a wide range of applications in research and industry. In spite of decades of study, the production of highly sensitive, homogeneous, reproducible, reusable, and cost-effective SERS substrates is still a big challenge. Two-dimensional (2D) nanomaterials which have many unique characteristics and properties provide new possibilities for SERS. For example, high Raman scattering has been observed from graphene.[2] When graphene is used to separate plasmonic metal particles and analyte molecules, both the signal and reproducibility of SERS could be improved.[3] Furthermore, graphene is highly impermeable, and could prevent the underlying silver (Ag) particles from oxidation at room temperature.[4] However, such protection is effective only in the short term,[5] and in the long run it actually speeds up oxidation as a result of galvanic corrosion.[6] In addition, graphene cannot solve the reusability challenge because it oxidizes at only 250 °C in air.[7]

Boron nitride (BN) nanosheets, atomically thin layers of hexagonal boron nitride (hBN), are another important member of 2D nanomaterials. BN nanosheets have mechanical strength, thermal conductivity, and impermeability similar to graphene, but are electrical insulators thermally stable up to 800 °C in air.[8] BN nanosheets could greatly contribute to SERS field. Take reusability as an example. It was found that thorough removal of adsorbed analyte molecules could, in most cases, be achieved only by heating treatments in oxygen or air but not by solvent washing.[9] Thus, to be reusable, SERS substrates need to withstand oxidation at high temperatures, which is especially difficult for oxidation-sensitive Ag nanoparticles. Traditional coatings, such as alumina (Al_2O_3), silica (SiO_2), and zinc oxide (ZnO_2) can increase the reusability of Ag nanoparticles,[10] but at the cost of dramatically reduced Raman enhancement: a 1.5 nm thick Al_2O_3 coating could reduce Raman enhancement by 75 %.[11] Another problem of ceramic coatings is their low affinity for most molecules, which means less number of molecules available for analysis, and hence weaker SERS signals. Atomically thin BN nanosheets can solve these problems. However, the use of atomically thin BN in SERS has been much less explored.[9b,12] More importantly, there still lack proof-of-concept studies to demonstrate the full potential of atomically thin BN in SERS application.

Herein, we show that atomically thin BN nanosheets can improve the sensitivity, reproducibility, and reusability of SERS substrates. The high flexibility makes atomically thin BN wrinkled to closely follow the contours of the underlying nanoparticles, with minimum decay of localized surface plasmon induced electromagnetic fields. Atomically thin BN has a stronger surface adsorption capability, and hence is more efficient in adsorption of analyte molecules at extremely low concentrations, resulting in dramatically improved sensitivity. Atomically thin BN is electrically insulating, so it can eliminate undesirable charge transfer as well as photocatalytic decomposition of analyte molecules to enhance reproducibility and stability of SERS. More importantly, atomically thin BN can protect Ag nanoparticles from oxidation in air even at high temperatures due to its high thermal stability and excellent impermeability. That is, the BN nanosheet covered SERS substrates have an outstanding reusability without loss of Raman enhancement.

[*] Q. Cai, S. Mateti, Prof. Y. Chen, Dr. L. H. Li
Institute for Frontier Materials
Deakin University
75 Pigdons Road, Waurn Ponds, 3216, VIC (Australia)
E-mail: ian.chen@deakin.edu.au
luhua.li@deakin.edu.au
Prof. W. Yang
Centre for Chemistry and Biotechnology, School of Life and Environmental Sciences, Deakin University
75 Pigdons Road, Waurn Ponds, 3216, VIC (Australia)
Dr. R. Jones
Department of Physics, La Trobe University
Bundoora, 3086, VIC (Australia)
Dr. K. Watanabe, Prof. T. Taniguchi
National Institute for Materials Science
Namiki 1-1, Tsukuba, Ibaraki 305-0044 (Japan)
Prof. S. Huang
Nanomaterials and Chemistry Key Laboratory, Wenzhou University
276 Xueyuan Middle Road, Wenzhou, Zhejiang, 325027 (China)

Supporting information for this article can be found under: http://dx.doi.org/10.1002/anie.201600517.

The high-quality BN nanosheets used in this study were mechanically exfoliated from hBN single crystals (see Supporting Information, Figure S2),[13] and rhodamine 6G (R6G), the most commonly used analyte for SERS analysis, was chosen as a model molecule. We first reveal the stronger surface-adsorption capability of atomically thin BN. After the BN nanosheets of different thicknesses were immersed in R6G aqueous solution of 10^{-6} M for 1 min, the atomic force microscopy (AFM) images (Figure 1 a,b) show that the thickness increase because of R6G adsorption for all the BN nanosheets was the same, that is, approximately 0.9 nm, corresponding to a monolayer of lying-down R6G molecules, whose xanthene ring structures are parallel to the BN surface as a result of strong π–π interactions.[14] However, the amount of the adsorbed molecules decreases with the increasing BN thickness. Such an intriguing phenomenon can be better seen in Figure 1 c, where the surface of all the BN nanosheets was adjusted to the same shade (i.e. AFM height) so that their coverage of R6G could be directly compared. The bilayer (2L) BN nanosheet was almost completely covered by R6G molecules, whereas the surface of a bulk hBN (ca. 50 nm thick) adsorbed far fewer molecules. Based on the AFM images,[15] the estimated adsorption coverage is 90 % on 2L BN, about 70 % on 3–6L BN, and less than 40 % on the bulk BN (Figure 1 d). Thus, the thinner the BN nanosheet, the higher the surface adsorption. According to our recent investigation, such phenomenon can be ascribed to conformational changes in atomically thin nanosheets, which increases adsorption energy and efficiency. Conformational changes often happen to soft adsorbates, such as macromolecules and biomolecules, and has been rarely observed on adsorbent. However, atomically thin BN nanosheets are highly flexible, so that the adsorbent, that is, the atomically thin BN, instead of adsorbate, R6G, experienced conformational changes in the current case. Bulk hBN crystals are not able to undergo conformational changes, so they have worse adsorption performance than atomically thin BN nanosheets.

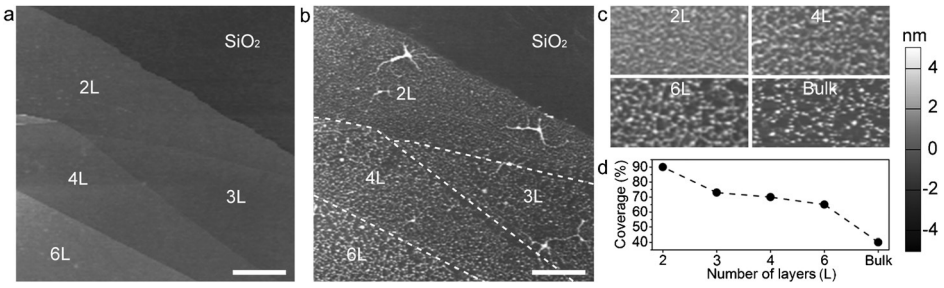

Figure 1. AFM images of BN nanosheets before (a) and after (b) R6G adsorption; c) normalized AFM images with the surface of BN of different thicknesses (number of layers (L)) adjusted to the same height to reveal the different coverage of adsorbed R6G molecules under the same adsorption conditions; d) estimated percentages of coverage versus BN thickness. Scale bars 2 μm.

The unique adsorption behavior and superior adsorption performance of atomically thin BN can improve the sensitivity of SERS. For this purpose, BN nanosheets were placed on top of plasmonic Ag nanoparticles, produced by thermal annealing of mechanically exfoliated BN nanosheets on sputtered Ag film on SiO_2/Si substrate (see Supporting Information for experimental details). As shown in Figure 2 a,b, the flexible 2L BN wrinkled to follow the profile of the underlying nanoparticles; thicker (17L) BN is more rigid and deformed to a much smaller degree (Figure 2 c,d). Their thicknesses (0.79 nm for 2L and 5.91 nm for 17L) were determined before annealing (Supporting Information, Figure S3). Figures 2 b,d show representative AFM height traces and the corresponding diagrams. The atomically thin and wrinkled 2L BN should give rise to stronger Raman enhancement than the 17L BN because plasmon-induced electromagnetic fields (i.e. hot spots) diminish exponentially with distance. In other words, atomically thin BN can better preserve the plasmonic hot spots. Note that the diameter and distribution of Ag nanoparticles with and without BN coverage are similar (see

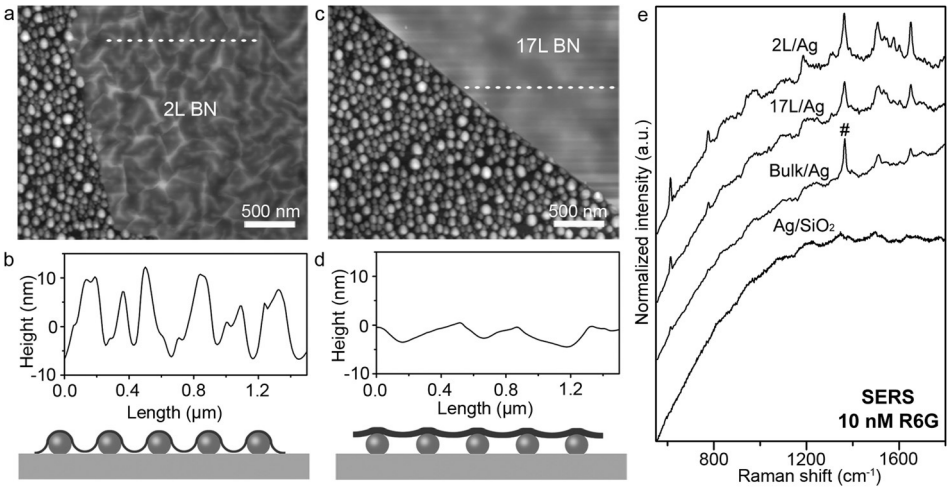

Figure 2. AFM images of Ag nanoparticles covered by 2L (a) and 17L (c) BN; b) and d) are the height traces and schematic diagrams along to the dotted lines in (a) and (c); e) SERS spectra of R6G (10 nM) from 2L, 17L, and bulk BN, as well as the Ag/SiO_2 substrate by adsorption method, and # indicates the Raman G band (E_{2g} mode) of bulk hBN.

Supporting Information, Figure S4), and according to our previous study, the dielectric constant of BN nanosheets of different thicknesses is quite close.[16]

The sensitivity of a bare Ag SERS substrate and the substrates veiled by BN nanosheets of different thicknesses was tested by immersing them in 10^{-8} M aqueous solution of R6G. As expected, the Raman features of R6G were most prominent from the 2L BN covered Ag nanoparticles (2L/Ag), and the signal attenuated with the increase of BN thickness (Figure 2e). The bare Ag nanoparticles on SiO_2/Si substrate (Ag/SiO_2), on the other hand, showed no Raman signature of R6G at either 10^{-8} or 10^{-7} M (Figure 2e and Supporting Information, Figure S5). That is, the 2L BN increased the sensitivity of the SERS substrates by more than two orders of magnitude. The much improved enhancement from the atomically thin BN covered SERS substrate can be largely attributed to the aforementioned two reasons: 1) atomically thin BN nanosheets were more efficient in the capture of analyte molecules, and 2) they better preserved Raman hot spots owing to their atomic thickness and wrinkles. Of these two causes, the first one played a decisive role because theoretically, the Ag/SiO_2 substrate should have the strongest electromagnetic field but showed no meaningful signal owing to its low affinity for aromatic molecules, whereas Bulk/Ag still showed weak Raman peaks of R6G (Figure 2e). This was further confirmed by estimating the enhancement factors of the different SERS substrates (see Supporting Information). Distinct from graphene which shows strong Raman peaks, the Raman yield of atomically thin BN is so weak that its G band is not visible. BN nanosheets can also improve SERS reproducibility and stability because they act as dielectric separators to prevent undesired decomposition of analyte molecules caused by the photocatalysis of Ag nanoparticles.

The homogeneity and reproducibility of the SERS substrates were checked by Raman mapping, as shown in Figure 3. The contrast of the Raman intensity in the areas with and without BN coverage is striking: the Ag/SiO_2 areas are mostly in black, indicating much weaker Raman sensitivity; whereas the signals from BN/Ag areas are several times stronger. In addition, the Raman enhancement from the BN areas is relatively homogeneous. The weaker Raman signals around the edges of the BN nanosheets should be due to the average of the signals from BN/Ag and Ag/SiO_2.

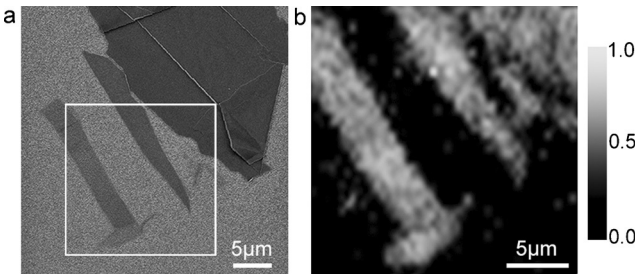

Figure 3. a) Scanning electron microscopy (SEM) image of Ag particles covered by BN of different thicknesses; b) the corresponding Raman mapping from the squared area in (a) after immersion in 10^{-6} M R6G solution for 1 h, where 0.0 indicates no intensity and 1.0 indicates the strongest measured Raman peak at 612 cm^{-1}.

Atomically thin BN nanosheets also make SERS substrates highly reusable. Heating in air has been found the most effective and efficient way to remove adsorbed organic molecules for reusable SERS.[9a,b] As shown in our previous studies,[6c,8] BN nanosheets are a promising barrier to protect metals because of their excellent thermal stability, high impermeability, and absence of galvanic corrosion. This means that the BN-covered Ag-based SERS substrates can have a long "shelf-time" without loss of sensitivity through oxidation, and more importantly, be regenerated by simply heating in air to burn off the adsorbed molecules and then reused. The reusability of 2L/Ag, Bulk/Ag, and Ag/SiO_2 substrates for up to 30 cycles are shown in Figure 4a–c. In each cycle, the substrate was heated at 360 °C in air, and then reused by immersion in R6G solution (10^{-6} M). The Raman signal and reusability of Ag/SiO_2 cannot be obtained at concentrations lower than 10^{-6} M. After the heating/cleaning treatment, no Raman signal of R6G was present on both 2L/Ag and Bulk/Ag samples, except a Si band at about 1000 cm^{-1} and/or G band of hBN at 1366 cm^{-1} (gray spectra in Figure 4a,b), implying effective removal of the analyte. After 30 cycles of reusability tests, the Raman intensity and frequency of R6G from 2L/Ag remained essentially unchanged (Figure 4a), indicating that the Ag nanoparticles were not affected even after the repeated heating in air. In comparison, the Raman enhancement from Bulk/Ag substrate slightly weakened with the increase of cycle numbers (Figure 4b). This difference can be attributed to the different morphologies of atomically thin and bulk hBN on Ag nanoparticles. Atomically thin BN nanosheets are so flexible that they wrinkled to better "seal" the underlying Ag nanoparticles from air; whereas thick hBN is unable to deform much, and there existed a gap between thick BN and SiO_2 substrate where air can penetrate to oxidize the Ag nanoparticles. Figure 2a–d, especially the lower traces, can be referred to visualize such difference. The Raman sensitivity of the bare Ag nanoparticles without BN protection, in contrast, plummeted in the reusability tests (Figure 4c). To better compare their different reusability, the Raman sensitivity of the three substrates after the tests are summarized in Figure 4f. The 2 L/Ag and Bulk/Ag substrates retained approximately 90 and 60% of their SERS activity after 30 cycles, respectively. For Ag/SiO_2, its plasmon enhancement decreased to 70% after the first cycle and further reduced to 20% after 7 cycles. Atomically thin BN also has a long-term protection on Ag nanoparticles: 2 L/Ag kept 90% of its Raman enhancement after exposure to ambient condition for 1 year; while the Ag/SiO_2 totally lost its enhancement (Supporting Information, Figure S7).

For comparison, we also tested the reusability of two representative coatings, namely Al_2O_3 and graphene, as both materials have been proposed as protective barriers for SERS substrates with Ag nanoparticles.[4a,10c] A 1.07 nm thick film (slightly thicker than 2L BN) of Al_2O_3 was grown on Ag/SiO_2 (Al_2O_3/Ag) by atomic layer deposition (ALD; see Supporting Information, Figure S8), which can produce highly dense and uniform thin films.[17] Al_2O_3/Ag showed Raman enhancement almost 10 times weaker than 2L/BN mainly for two reasons. First, Al_2O_3 has a low affinity for R6G so that much fewer

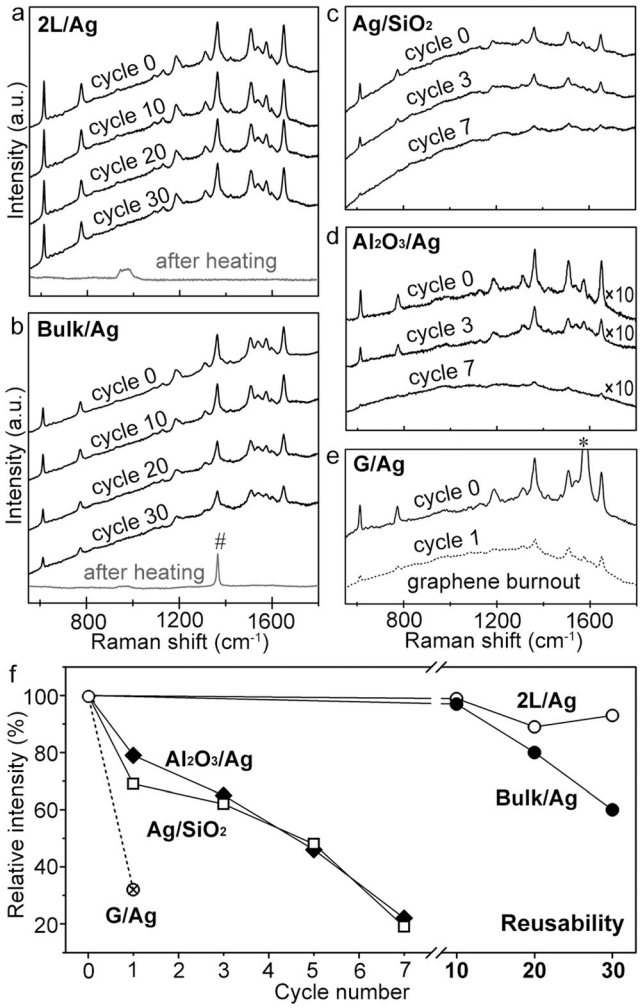

Figure 4. Reusability tests of different SERS substrates: a) 2L BN covered Ag nanoparticles (2L/Ag) for 30 cycles (in each cycle, the substrate was heated at 360 °C in air for 5 min and re-immersed in 10^{-6} M R6G solution); b) bulk BN on Ag nanoparticles (Bulk/Ag) for 30 cycles, where # indicates the G band of bulk hBN; the gray spectra in (a,b) are after heating without re-immersion; c) bare Ag particles on SiO_2 without BN protection (Ag/SiO_2) for 7 cycles; d) ca. 1 nm thick ALD Al_2O_3 on Ag nanoparticles (Al_2O_3/Ag), and e) 10 nm thick graphene on Ag nanoparticles (G/Ag) for 1 cycle, where * indicates the G band of graphite. The SERS spectra in (a)–(e) are vertically offset for clarity. f) Summarizes the change of the Raman enhancement of these SERS substrates based on the intensity of the 612 cm^{-1} peak.

amounts of molecules can be adsorbed on the substrate. Second, it was reported that a 1.5 nm thick Al_2O_3 film can reduce the Raman enhancement by more than 75%.[11] Moreover, the Al_2O_3 film showed almost no protection which could be due to the inevitable defects in the film (Figure 4d), and its enhancement dropped to 20% after 7 cycles of reusability test, following a similar trend of Ag/SiO_2 (Figure 4f).

High-quality graphene of 10 nm was produced on Ag nanoparticles by mechanical exfoliation, following the same synthesis route of BN/Ag. The SERS substrate of graphene covered Ag nanoparticles (G/Ag) showed comparable Raman enhancement to that of Bulk/Ag because graphene can also attract R6G via π–π interaction, but with lower background owing to charge transfer (Figure 4e).[2a,18] The G band of graphene (labeled by *) is pronounced compared to the peaks from R6G. The heating at 360 °C in air for 5 min (1 cycle) had a disastrous effect on the Raman enhancement of G/Ag with a drop to 30% of the initial signal strength (dashed line in Figure 4f). It was because the around 10 nm thick graphene burnt out after the heating treatment (see Supporting Information, Figure S9), which dramatically decreased the amount of R6G molecules adsorbed on bare Ag/SiO_2 without graphene.

X-ray photoelectron spectroscopy (XPS) was used to analyze the oxidation levels of Ag nanoparticles on these substrates after reusability tests (Figure 5). Ag nanoparticles

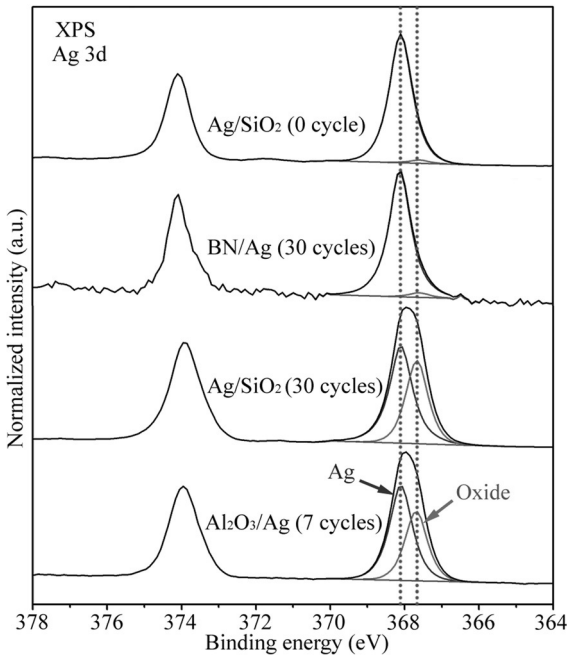

Figure 5. XPS spectra of Ag particles with and without BN protection before and after reusability tests. Dotted lines mark the positions of the signals arising from silver and silver oxide.

protected by BN nanosheets showed a dominating silver peak at 368.2 eV, indicating almost no increase of silver oxide after 30 cycles of reusability tests; while Ag particles without protection of BN or covered by the Al_2O_3 thin film showed a strong silver oxide peak at 367.6 eV,[19] suggesting an oxide content of about 50% after reusability tests. These results further confirm that BN nanosheets are an excellent material for reusable SERS devices.

In summary, atomically thin BN nanosheets can be used to fabricate highly sensitive, reproducible, and reusable SERS substrates. They are efficient in adsorption of aromatic molecules to improve Raman sensitivity, especially at extremely low concentrations. The Raman enhancement from such substrates was homogeneous and reproducible. Furthermore, BN nanosheets could provide the Ag nanoparticles with long-term protection from oxidation even at high temperatures in air so that excellent reusability was

achieved. The proposed SERS substrate and fabrication method can be easily scaled up using large-sized BN nanosheets grown by chemical vapor deposition (CVD).[20] On the other hand, BN nanosheets can be also used to cover SERS substrates produced by other methods, for example, self-assembly, or other metal nanoparticles to improve surface adsorption, reproducibility, and reusability.

Acknowledgements

L.H.L. thanks the financial support from the Australian Research Council under Discovery Early Career Researcher Award (DE160100796), and Deakin University under Alfred Deakin Research Postdoctoral Fellowship 2014, and Central Research Grants Scheme 2015. Y.C. acknowledges the funding support from the Australian Research Council under the Discovery project. We also thank the funding from NSFC No. 51420105002. This work was performed in part at the Melbourne Centre for Nanofabrication (MCN).

Keywords: boron nitride · nanosheets · silver · surface adsorption · surface enhanced Raman spectroscopy (SERS)

How to cite: *Angew. Chem. Int. Ed.* **2016**, *55*, 8405 – 8409
Angew. Chem. **2016**, *128*, 8545 – 8549

[1] a) S. Schlücker, *Angew. Chem. Int. Ed.* **2014**, *53*, 4756 – 4795; *Angew. Chem.* **2014**, *126*, 4852 – 4894; b) P. H. C. Camargo, M. Rycenga, L. Au, Y. N. Xia, *Angew. Chem. Int. Ed.* **2009**, *48*, 2180 – 2184; *Angew. Chem.* **2009**, *121*, 2214 – 2218.

[2] a) X. Ling, L. M. Xie, Y. Fang, H. Xu, H. L. Zhang, J. Kong, M. S. Dresselhaus, J. Zhang, Z. F. Liu, *Nano Lett.* **2010**, *10*, 553 – 561; b) X. Ling, J. Zhang, *Small* **2010**, *6*, 2020 – 2025; c) H. H. Cheng, Y. Zhao, Y. Q. Fan, X. J. Xie, L. T. Qu, G. Q. Shi, *ACS Nano* **2012**, *6*, 2237 – 2244; d) Z. Y. Zhang, Q. H. Liu, D. L. Gao, D. Luo, Y. Niu, J. Yang, Y. Li, *Small* **2015**, *11*, 3000 – 3005.

[3] a) W. Xu, J. Xiao, Y. Chen, Y. Chen, X. Ling, J. Zhang, *Adv. Mater.* **2013**, *25*, 928 – 933; b) W. Xu, X. Ling, J. Xiao, M. S. Dresselhaus, J. Kong, H. Xu, Z. Liu, J. Zhang, *Proc. Natl. Acad. Sci. USA* **2012**, *109*, 9281 – 9286; c) Z. Zhang, F. G. Xu, W. S. Yang, M. Y. Guo, X. D. Wang, B. L. Zhanga, J. L. Tang, *Chem. Commun.* **2011**, *47*, 6440 – 6442; d) P. Luo, C. Li, G. Shi, *Phys. Chem. Chem. Phys.* **2012**, *14*, 7360 – 7366; e) J. Wang, X. Gao, H. Sun, B. Su, C. Gao, *Mater. Lett.* **2016**, *162*, 142 – 145.

[4] a) X. Li, J. Li, X. Zhou, Y. Ma, Z. Zheng, X. Duan, Y. Qu, *Carbon* **2014**, *66*, 713 – 719; b) M. Losurdo, I. Bergmair, B. Dastmalchi, T. H. Kim, M. M. Giangregroio, W. Y. Jiao, G. V. Bianco, A. S. Brown, K. Hingerl, G. Bruno, *Adv. Funct. Mater.* **2014**, *24*, 1864 – 1878.

[5] a) D. Prasai, J. C. Tuberquia, R. R. Harl, G. K. Jennings, K. I. Bolotin, *ACS Nano* **2012**, *6*, 1102 – 1108; b) S. Chen, L. Brown, M. Levendorf, W. Cai, S.-Y. Ju, J. Edgeworth, X. Li, C. W. Magnuson, A. Velamakanni, R. D. Piner, *ACS Nano* **2011**, *5*, 1321 – 1327.

[6] a) F. Zhou, Z. Li, G. J. Shenoy, L. Li, H. Liu, *ACS Nano* **2013**, *7*, 6939 – 6947; b) M. Schriver, W. Regan, W. J. Gannett, A. M. Zaniewski, M. F. Crommie, A. Zettl, *ACS Nano* **2013**, *7*, 5763 – 5768; c) L. H. Li, T. Xing, Y. Chen, R. Jones, *Adv. Mater. Interfaces* **2014**, *1*, 1300132.

[7] L. Liu, S. M. Ryu, M. R. Tomasik, E. Stolyarova, N. Jung, M. S. Hybertsen, M. L. Steigerwald, L. E. Brus, G. W. Flynn, *Nano Lett.* **2008**, *8*, 1965 – 1970.

[8] L. H. Li, J. Cervenka, K. Watanabe, T. Taniguchi, Y. Chen, *ACS Nano* **2014**, *8*, 1457 – 1462.

[9] a) P. Aldeanueva-Potel, E. Faoucher, R. A. Alvarez-Puebla, L. M. Liz-Marzan, M. Brust, *Anal. Chem.* **2009**, *81*, 9233 – 9238; b) Y. Lin, C. E. Bunker, K. S. Fernando, J. W. Connell, *ACS Appl. Mater. Interfaces* **2012**, *4*, 1110 – 1117; c) S. Faraji, K. L. Stano, O. Yildiz, A. Li, Y. Zhu, P. D. Bradford, *Nanoscale* **2015**, *7*, 17038 – 17047.

[10] a) X. Y. Zhang, J. Zhao, A. V. Whitney, J. W. Elam, R. P. Van Duyne, *J. Am. Chem. Soc.* **2006**, *128*, 10304 – 10309; b) J. F. Li, Y. F. Huang, Y. Ding, Z. L. Yang, S. B. Li, X. S. Zhou, F. R. Fan, W. Zhang, Z. Y. Zhou, D. Y. Wu, B. Ren, Z. L. Wang, Z. Q. Tian, *Nature* **2010**, *464*, 392 – 395; c) S. M. Mahurin, J. John, M. J. Sepaniak, S. Dai, *Appl. Spectrosc.* **2011**, *65*, 417 – 422; d) L. W. Ma, Y. Huang, M. J. Hou, Z. Xie, Z. J. Zhang, *Sci. Rep.* **2015**, *5*, 12890.

[11] J. A. Dieringer, A. D. McFarland, N. C. Shah, D. A. Stuart, A. V. Whitney, C. R. Yonzon, M. A. Young, X. Y. Zhang, R. P. Van Duyne, *Faraday Discuss.* **2006**, *132*, 9 – 26.

[12] a) X. Ling, W. Fang, Y.-H. Lee, P. T. Araujo, X. Zhang, J. F. Rodriguez-Nieva, Y. Lin, J. Zhang, J. Kong, M. S. Dresselhaus, *Nano Lett.* **2014**, *14*, 3033 – 3040; b) P. Dai, Y. Xue, X. Wang, Q. Weng, C. Zhang, X. Jiang, D. Tang, X. Wang, N. Kawamoto, Y. Ide, *Nanoscale* **2015**, *7*, 18992 – 18997.

[13] a) T. Taniguchi, K. Watanabe, *J. Cryst. Growth* **2007**, *303*, 525 – 529; b) L. Li, L. H. Li, Y. Chen, X. J. Dai, P. R. Lamb, B. M. Cheng, M. Y. Lin, X. Liu, *Angew. Chem. Int. Ed.* **2013**, *52*, 4212 – 4216; *Angew. Chem.* **2013**, *125*, 4306 – 4310.

[14] Q. Cai, L. H. Li, Y. Yu, Y. Liu, S. Huang, Y. Chen, K. Watanabe, T. Taniguchi, *Phys. Chem. Chem. Phys.* **2015**, *17*, 7761 – 7766.

[15] L. H. Li, Y. Chen, *Langmuir* **2010**, *26*, 5135 – 5140.

[16] L. H. Li, E. J. Santos, T. Xing, E. Cappelluti, R. Roldán, Y. Chen, K. Watanabe, T. Taniguchi, *Nano Lett.* **2015**, *15*, 218 – 223.

[17] M. Knez, N. Pinna, Wiley-VCH, Wiley, Weinheim, Chichester, **2011**.

[18] E. S. Thrall, A. C. Crowther, Z. H. Yu, L. E. Brus, *Nano Lett.* **2012**, *12*, 1571 – 1577.

[19] a) E. Albiter, M. Valenzuela, S. Alfaro, G. Valverde-Aguilar, F. Martínez-Pallares, *J. Saudi Chem. Soc.* **2015**, *19*, 563 – 573; b) E. Mysak, J. Smith, P. Ashby, J. Newberg, K. Wilson, H. Bluhm, *Phys. Chem. Chem. Phys.* **2011**, *13*, 7554 – 7564.

[20] a) Y. M. Shi, C. Hamsen, X. T. Jia, K. K. Kim, A. Reina, M. Hofmann, A. L. Hsu, K. Zhang, H. N. Li, Z. Y. Juang, M. S. Dresselhaus, L. J. Li, J. Kong, *Nano Lett.* **2010**, *10*, 4134 – 4139; b) L. Song, L. J. Ci, H. Lu, P. B. Sorokin, C. H. Jin, J. Ni, A. G. Kvashnin, D. G. Kvashnin, J. Lou, B. I. Yakobson, P. M. Ajayan, *Nano Lett.* **2010**, *10*, 3209 – 3215; c) Y. Gao, W. C. Ren, T. Ma, Z. B. Liu, Y. Zhang, W. B. Liu, L. P. Ma, X. L. Ma, H. M. Cheng, *ACS Nano* **2013**, *7*, 5199 – 5206.

Received: January 17, 2016
Published online: April 26, 2016

